

Hybrid single mode lasers fabricated using Si/SiO₂/SiON micromachined platforms

A. Ksendzov*, K. Mansour

Jet Propulsion Laboratory, California Institute of Technology, 4800 Oak Grove Drive, Pasadena, CA 91109

ABSTRACT

We have devised a hybridization scheme that, given suitable Fabri-Perot (F-P) gain medium, allows us to fabricate small, mechanically robust single frequency lasers in a wide spectral range, limited only by the transparency of the SiON material. In this report we discuss device fabrication and present characteristics of a laser emitting in red spectral range. The laser operates at or near room temperature under continuous wave excitation and emits 5 mW of power in single mode with 40 dB side mode suppression.

Keywords: lasers, hybridization, integrated optics, sensors

INTRODUCTION

The early work on narrow linewidth semiconductor lasers utilized the hybrid approach [1]. The emphasis was on the device physics rather than manufacturability. A number of more recent reports dealt with the coupling of lasers to a planar lightguide circuit (PLC) [2]. These PLCs utilize $6 \times 6 \mu\text{m}^2$ silica waveguides and require lasers with spot size converters for the efficient coupling of light. Such lasers are not readily available, especially at wavelengths outside fiberoptic communication bands. In contrast, our technique is applicable to the simple cleaved F-P gain chips without spot size converters. The technology is within the scope of a typical silicon fabrication facility. It is attractive for satisfying the needs of specialty applications such as interferometric metrology or gas detection that may require operation outside the typical communication wavelengths. Other possible applications include integrated optical sensors and tunable lasers.

FABRICATION TECHNIQUE

Our hybrid devices are essentially distributed Bragg reflector (DBR) lasers with external Bragg gratings defined in SiO₂/SiON/SiO₂ waveguide structures. The waveguide structure is an integral part of a

SiO₂/SiON/SiO₂ micromachined platform defined on a silicon substrate. The top view of a laser comprising a gain chip and the platform is provided in Figure 1. The light output is taken from the gain chip facet on the left side of Figure 1.

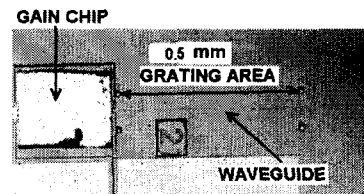


Figure 1. Assembled hybrid laser.

The 500 μm long gain chips were acquired from SLI Corp. and are their standard F-P product. For efficient coupling the external waveguide was designed to have a mode similar to the gain chip mode with an approximate size of $2.5 \times 0.5 \mu\text{m}^2$. In addition, the chip must be precisely aligned to the external waveguide. To that end, the micromachined platform provides the features facilitating vertical alignment. The lateral alignment was accomplished with a precision flip chip bonder. The Bragg grating starts immediately to the right of the gain chip.

The waveguide stack was deposited by the plasma enhanced chemical vapor deposition (PECVD) on an oxidized Si wafer (wet oxide 5 μm thick) - first the bottom SiO₂ cladding ($n=1.458$), and then 0.5 μm SiON

* alexander.ksendzov@jpl.nasa.gov

core ($n=1.571$). Then the Bragg grating was defined by direct electron beam write in polymethylmethacrylate resist and transferred onto the core using ion milling. The grating is 0.5 mm long. A typical grating etch profile is shown in Figure 2.

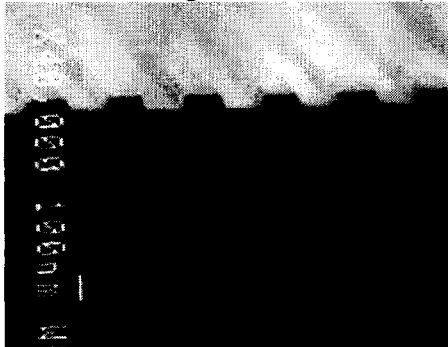


Figure 2. Scanning electron microscope image of a grating cross section.

In the next step, the 0.06 μm tall, 2 μm wide rib waveguide was defined by reactive ion etching (RIE) to provide lateral confinement. The waveguide cross section is depicted in Figure 3A. Then the 1.5 μm thick top SiO_2 cladding was deposited by PECVD.

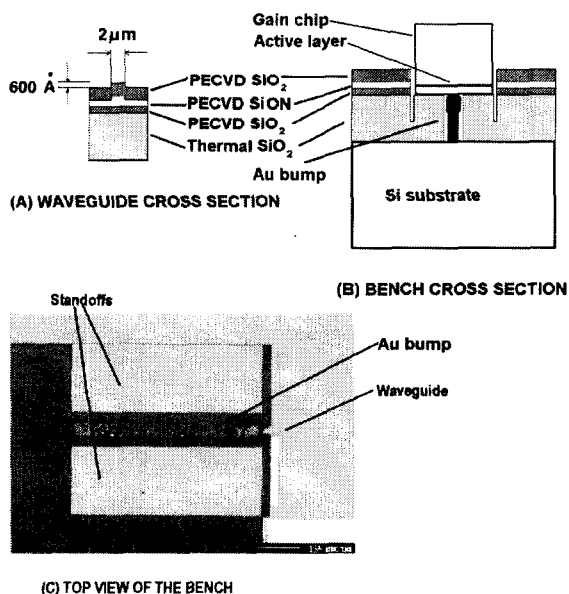


Figure 3. (A) Waveguide cross section, (B) The micromachined bench cross section with the gain chip mounted, and (C) The micromachined bench – top view.

The cross section of the micromachined bench is pictured in Figure 3B. The main feature of the bench is the precise definition of the vertical distance between

stand-offs and the waveguide core. This was accomplished by defining Cr etch stops prior to the lower cladding deposition by PECVD. The vertical distance between the stand-offs and the core is thus defined by the deposition rate and can be easily controlled with 0.1 μm accuracy. This dimension is critical for the proper vertical alignment of the gain chip (see Figure 3B). The deep recess was produced using RIE. The Cr etch stops were then removed by wet etching and the wafer was annealed at 1100 $^{\circ}\text{C}$ to densify the PECVD material.

The top view photograph of the micromachined platform is presented in Figure 3C. The chip was attached to the bench p-side down (flip-chip configuration) using a soft Au bump (see Figs. 3B and 3C). The bump was defined by electroplating as a 12 μm wide 500 μm long stripe and was designed to be 2-3 μm taller than standoffs. It was squashed during the bonding process down to the stand-off level to facilitate a strong bond. Horizontal alignment was achieved using a high precision flip-chip bonder. We used Finetech Lambda Placer Bonder with heated top and bottom chucks. Both chucks were held at 375 $^{\circ}\text{C}$ during the bonding cycle.

COMPONENT CHARACTERIZATION

We have characterized the gain chip and the Bragg grating used for the laser prior to hybridization. The gain chip received an antireflection coating on the facet to be coupled into the Bragg grating. The other facet was coated to achieve 40% reflectance. Both coatings were deposited by the die manufacturer.

The Bragg grating transmittance was measured before the wafer was diced. The light from a tunable diode laser was coupled into the edge of the waveguide. To achieve precise wavelength readings a wavelength meter was utilized during the scan. The light propagation was imaged by a CCD camera (in top view) and the grating transmittance was evaluated by comparing the intensity of light entering and leaving the grating area. The wavelength scan and data acquisition were controlled by a computer. The transmittance spectrum of the Bragg grating is presented in Figure 4A.

The net gain was evaluated using the expression derived by Cassidy [3]. Assuming the antireflection coating is perfect and the reflectance of the other facet is R , the single pass gain G can be expressed as

$$G(\lambda) = \frac{1 - R - r(\lambda)}{r(\lambda)R}, \quad (1)$$

where r is the ratio of light intensities emitted from the two facets and λ is the wavelength of light. The unmounted gain chip was excited by pulsed current to avoid heating effects. Output from each of the facets was measured by coupling the light into a spectrometer using

high numerical aperture multimode fiber. The results obtained using expression (1) are plotted in Figure 4B. These measurements indicated good overlap between the central area of the gain curve and the maximum of the optical feedback.

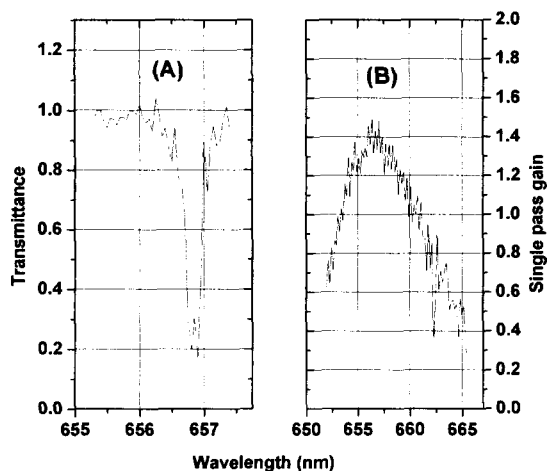


Figure 4. (A) Transmittance of the Bragg grating. (B) Single pass gain measured at room temperature using 30 mA pulsed current.

RESULTS AND DISCUSSION

The emission spectrum of the laser recorded with an optical spectrum analyzer is presented in Figure 6. The spectrum was taken at 10 °C using continuous wave (CW) excitation. The laser current was set to 86 mA and the analyzer bandwidth was set to 0.06 nm. The laser operated in single mode regime with 40 dB side mode suppression. The single mode regime persisted through a wide range of temperatures (10 to 30 °C) and currents (65 to 90 mA).

The light-current curve of the laser taken at 10 °C is presented in Figure 7B. The threshold current is approximately 60 mA. The notches on the curve stem from the mode hops observed previously in red DBR lasers [2, 4]. They are accompanied by abrupt changes in wavelength as seen in the wavelength vs. current plot (Figure 7A).

The ability to control the emission wavelength is important in metrology and gas sensing applications. Since temperature tuning is one of the simplest ways to achieve such control, we have measured the temperature dependence of the emission wavelength. The results shown in Figure 8 were obtained at 76 mA (CW). The dependence reflects two trends: the repeated saw-tooth like behavior with a slope of approximately 4×10^{-2} nm/K

superimposed on a slower 'envelope' (dotted lines in Figure 8) with a slope of approximately 7×10^{-3} nm/K.

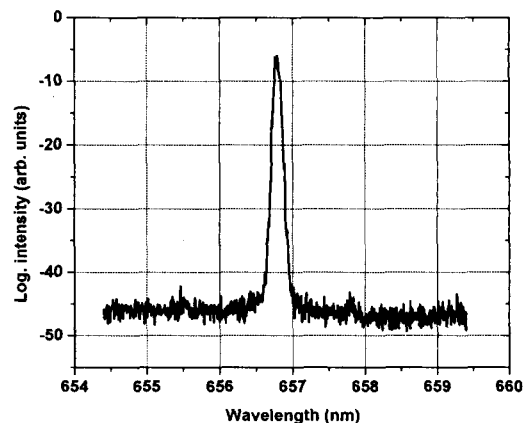


Figure 6. The laser emission spectrum recorded at 10 °C.

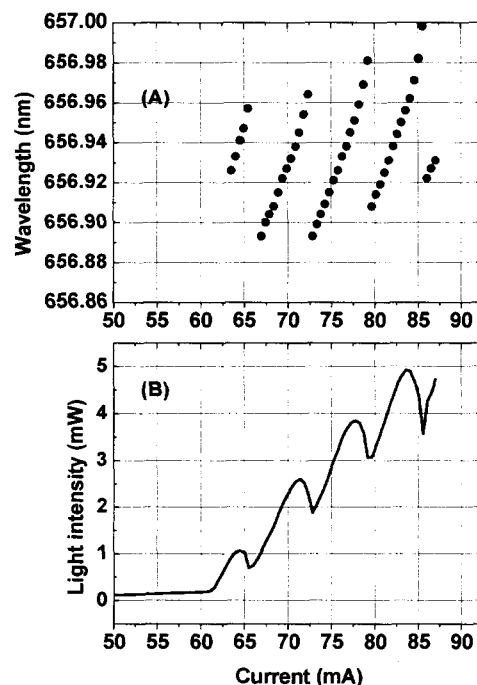


Figure 7. (A) Plot of emission wavelength vs. current. (B) Plot of laser power vs. current. Measurements were done at 10 °C.

We have the following interpretation of this measurement. The fast component presumably results from the shift of the operating point along the short wavelength slope of the Bragg grating reflectance curve, caused by the change in the refractive index of the gain medium. The detailed discussion of the operating point

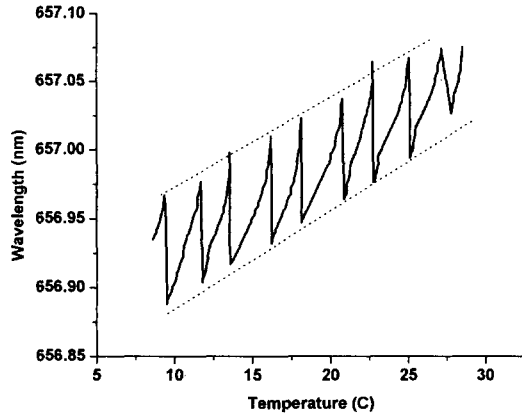


Figure 8. Plot of emission wavelength vs. temperature. Solid lines represent the measurement result. Dotted lines are drawn as a guide to outline the envelope.

for lasers with external feedback was given by Kazarinov et al⁵. The slow 'envelope' component comes from the shift of the grating frequency with temperature. It is consistent with the temperature variation of the optical path length in similar waveguides measured in our laboratory.

CONCLUSION

In conclusion, we introduced a hybridization technique that allows fabrication of single mode lasers in wide spectral range limited only by the transparency region of SiON material. Unlike previous reports, the technique requires only the simplest Fabri-Perot gain medium and can be implemented in a typical silicon fabrication facility. This fabrication method can be used to satisfy requirements of low volume applications such as optical metrology or gas sensing. We have demonstrated the technique using a 650 nm gain medium.

ACKNOWLEDGEMENTS

This research was carried out at the Jet Propulsion Laboratory, California Institute of Technology, under a contract with the National Aeronautics and Space Administration. The authors thank Dr. Siamak Forouhar for valuable discussions and advice.

REFERENCES

1. N.A. Olsson, C.H. Henry, R.F. Kazarinov, H.J. Lee, K.J. Orlowsky, B.H. Johnson, R.E. Scotti, D.A. Ackerman, and P.J. Anthony. 'Performance characteristics of a 1.5 μm single frequency semiconductor laser with an external waveguide Bragg reflector', IEEE Journ. of Quantum Electronics, 1988 24 (2) pp. 143-147.
2. T. Tanaka, H. Takahashi, Y. Hibino, T. Hashimoto, A. Himeno, Y. Yamada, and Y. Tohomori. 'Hybrid external cavity lasers composed of spot-size converter integrated LDs and UV written Bragg gratings in a planar waveguide Circuit on Si', IEICE Trans. Electron. 2000, E83-C (6) pp. 875-883.
3. D.T. Cassidy. 'Technique for measurement of gain spectra of semiconductor diode lasers', J. Appl. Phys. 1984, 56 (11) pp. 3096-3099.
4. B. Pezeshki, J.S. Osinski, H. Zhao, A. Mathur and T.L. Koch. 'GaInP/AlGaInP 670 nm singlemode DBR laser', Electronics Letters 1996, 32 (24) pp. 2241-2243.
5. R.F. Kazarinov and C.H. Henry. 'The relation of line narrowing and chirp reduction resulting from the coupling of a semiconductor laser to a passive resonator', J. of Quant. Electronics 1987 Q-23 (9) pp. 1401-1409.